

# Losing the maternal effect gene *Nlrp2* alters the ovulated mouse oocytes transcriptome and impacts histone demethylase KDM1B expression

**Zahra Anvar**

Baylor College of Medicine

**Imen Chakchouk**

Baylor College of Medicine

**Momal Sharif**

Baylor College of Medicine

**Sangeetha Mahadevan**

Baylor College of Medicine

**Eleni Theodora Nasiotis**

Baylor College of Medicine

**Li Su**

Baylor College of Medicine

**Zhandong Liu**

Baylor College of Medicine

**Ying-Wooi Wan**

Texas Children's Hospital

**Ignatia B. Veyver** (✉ [iveyver@bcm.edu](mailto:iveyver@bcm.edu))

Baylor College of Medicine

---

## Article

**Keywords:** subcortical maternal complex, NLRP2, oocyte, RNA sequencing

**Posted Date:** September 16th, 2022

**DOI:** <https://doi.org/10.21203/rs.3.rs-2042545/v1>

**License:**  This work is licensed under a Creative Commons Attribution 4.0 International License. [Read Full License](#)

---

## Abstract

The subcortical maternal complex (SCMC) is a multiprotein complex in oocytes and preimplantation embryos that is encoded by maternal effect genes. The SCMC is essential for zygote-to-embryo transition, early embryogenesis, and critical zygotic cellular processes like spindle positioning and symmetric division. Maternal deletion of *Nlrp2*, which encodes an SCMC protein, results in increased early embryonic loss and abnormal DNA methylation in embryos. We performed RNA sequencing on pools of oocytes that we isolated and collected from cumulus-oocyte complexes (COCs) after inducing ovarian stimulation in wild-type and *Nlrp2*-null female mice. Using a mouse reference genome-based analysis, we found 231 differentially expressed genes (DEGs) in *Nlrp2*-null compared to WT oocytes (123 up- and 108 downregulated; adjusted  $p < 0.05$ ). The DEGs we identified were enriched for processes involved in neurogenesis, gland morphogenesis, and protein metabolism and for post-translationally methylated proteins. When we compared our RNA sequencing results to an oocyte-specific reference transcriptome that contains many previously unannotated transcripts, we found 228 DEGs, including genes not identified with the first analysis. Intriguingly, 68% and 56% of DEGs from the first and second analyses, respectively, overlap with oocyte-specific hyper- and hypomethylated domains. Thus, the differentially expressed transcripts in the oocytes of mice lacking NLRP2 are enriched for genes that overlap with oocyte-specific methylated domains. This is consistent with the known functional link between transcription and methylation in oocytes.

## Introduction

During the earliest divisions of preimplantation embryonic development, before the zygotic genome is activated, transcription is quiescent and depends on how stored RNAs and proteins expressed from maternal effect genes act during oocyte development. The proteins that maternal effect genes encode abound in oocytes and early preimplantation embryos and play essential roles in early embryo development<sup>1</sup>. The subcortical maternal complex (SCMC) is a multiprotein complex localized below the cortex of oocytes that contain proteins encoded by maternal effect genes. The SCMC sits on the periphery of the preimplantation embryo during its earliest cell divisions but gradually decreases in number after fertilization and, in mice, it is no longer visible by the blastocyst stage<sup>2,3</sup>. Eight SCMC proteins have been identified so far: OOEP (previously known as FLOPED), NLRP5, TLE6, KHDC3 (previously known as FILIA), ZBED3, NLRP2, PADI6, and NLRP4<sup>2,4-9</sup>. The SCMC is involved in multiple cellular processes, including controlling spindle position, symmetric zygote division, organelle distribution, and cytoplasmic lattice formation<sup>6,10-13</sup>.

Studies in mice have shown that maternal loss of function in genes that encode SCMC proteins causes sterility or subfertility. Targeted disruption of maternal *Ooep*, *Nlrp5*, *Padi6*, or *Tle6* results in complete embryonic arrest at the two-cell or early cleavage stages<sup>2,7,10,14,15</sup>. Although maternal loss of *Khdc3*, *Zbed3*, or *Nlrp2* also leads to delayed preimplantation development and reduced fertility, it can be compatible with later embryo development, and even with survival after birth in a small number of offspring<sup>6,16,17</sup>.

SCMC genes and proteins are highly conserved in mammals. In humans, women with biallelic inactivating mutations in *NLRP7* (which is not present in rodent genomes), *KHDC3L*, and *PADI6* develop biparental complete hydatidiform mole (BiCHM), which manifests in an abnormal pregnancy characterized by chorionic villi overproliferation and lack of embryonic/fetal tissue<sup>18-21</sup>. Molar trophoblast tissues lack allelic methylation at imprinted loci, including those with placenta-specific imprinted differentially methylated regions (DMRs)<sup>22</sup>. The recent finding that oocytes from a BiCHM patient with a homozygous inactivating mutation in maternal *KHDC3L* had a genome-wide DNA methylation loss that persisted at imprinted loci until post-implantation confirmed that the methylation defect's origin is in the female germline<sup>23</sup>.

Loss of several other SCMC genes (*NLRP5*, *NLRP2*, *NLRP7*, *PADI6*, *OOEP*, and *KHDC3L*) in humans also causes multilocus imprinting disturbance (MLID), in which DNA methylation is lost at multiple maternally imprinted loci which results in recurrent pregnancy loss and offspring with complex imprinting disorders<sup>24-28</sup>. We previously reported that maternal loss of *Nlrp2* in mice causes subfertility with variable reproductive outcomes ranging from early embryonic loss to stillborn pups to, rarely, live-born offspring with myriad developmental defects. We also found altered methylation at selected imprinted genes' differentially methylated regions (DMRs)<sup>16</sup>.

The mechanism by which cytoplasmic SCMC disruption affects DNA methylation—a nuclear process—remains poorly understood. Our observations, above, suggest that the SCMC may have an epigenetic regulatory role. It may directly affect the epigenetic machinery or disrupt different oocyte functions which could in turn globally alter the transcriptome.

In human and mouse oocytes, transcription drives the establishment of DNA methylation<sup>29–32</sup>, and in mice, transcriptional aberrations disrupt oocyte-derived methylation<sup>33</sup>. Thus, we hypothesized that transcriptional changes should occur in *Nlrp2*-null female oocytes and that these might underlie methylation defects in oocytes, embryos, or offspring. We began investigating this by performing RNA sequencing (RNA-Seq) on pooled oocytes isolated from cumulus-oocyte complexes (COCs) collected after *Nlrp2* female superovulation. Our results showed that maternal *Nlrp2* loss globally alters the oocyte transcriptome.

## Results

### Differentially expressed genes (DEGs) in *Nlrp2*-null compared to WT oocytes

We isolated meiosis II (MII) oocytes from superovulated wild-type (WT) and *Nlrp2*-null female mice's COCs. To profile the oocyte transcriptomes for both genotypes and examine changes in transcript abundance caused by maternal loss of *Nlrp2*, we performed RNA-Seq on pools of ~150 oocytes, including three pools from WT and four pools from *Nlrp2*-null females (Fig. 1). We first analyzed the RNA-Seq data by aligning obtained sequences to the mouse reference genome. After filtering out genes that were covered by fewer than 10 average read counts, we retained 18,951 genes for further analysis. We performed principal component analysis (PCA) to characterize the internal group separation, detect any outliers, and determine the degree of variation between WT and *Nlrp2*-null samples and between replicates for each. This showed that transcriptome data from the four *Nlrp2*-null pools clustered with each other and separated from the WT pool data (Fig. 2a). We then used DESeq to find differentially expressed genes (DEGs) between the WT and *Nlrp2*-null oocyte pools, which yielded 231 DEGs (adjusted p-value < 0.05) (Supplementary Table 1). Of these, 123 were upregulated and 108 were downregulated in *Nlrp2*-null oocyte pools (Fig. 2b).

### Altered biological processes and pathways in *Nlrp2*-null oocytes

We next analyzed the biological functions of the 231 genes that are differentially expressed between *Nlrp2*-null and WT oocyte pools. Based on Database for Annotation, Visualization, and Integrated Discovery (DAVID) analysis<sup>34–36</sup> (Table 1), both neurogenesis and differentiation were enriched among genes with altered expression in *Nlrp2*-null oocytes. Within the differentiation category, the main enriched terms were multicellular organism development, nervous system development, and axon guidance. There were two significantly enriched molecular function categories: (1) developmental protein, which included significant multicellular organism development and nervous system development subcategories, and (2) chaperone, which included significant enrichment of four subcategories (ATPase activity, protein processing in the endoplasmic reticulum, positive regulation of telomerase activity, and COP9 signalosome). Enriched cellular components included cytoplasm and tight junction. Enriched tight junctions included cell adhesion molecules, bicellular tight junction, cell junction, and cell-cell adhesion. We performed functional analysis using the WEB-based Gene SeT Analysis Toolkit (WebGestalt)<sup>37</sup> (Table 2) for enriched biological processes (with p-value < 0.05 and FDR < 0.05) and found the following enriched processes: protein metabolism, gland morphogenesis, post-translational protein modification, the cell morphogenesis that occurs during neuron differentiation, axonogenesis, plasma membrane-bounded cell projection organization, cellular protein localization, cellular macromolecule localization, cell projection organization, and neuron projection morphogenesis pathways. The Search Tool for the Retrieval of Interacting Genes/Proteins (STRING)<sup>38</sup> (Table 3) revealed the following top 10 enriched pathways: gland morphogenesis, biological regulation, cellular process regulation, axonogenesis, neuron projection morphogenesis, biological process regulation, cell morphogenesis that occurs during neuron differentiation, regulation of cellular response to growth factor stimulus, multicellular organism development, and neuron differentiation. Enrichments that all three tools (DAVID, WebGestalt, and STRING analysis) (Table 1–3) identified include processes and pathways involved with neurogenesis, nervous system development, axonogenesis, axon guidance, cell morphogenesis that occurs during neuron differentiation, and neuron projection morphogenesis. Interestingly, scientists observed neurogenesis enrichment in another study that evaluated DNA methylation in meiosis II (MII) stage oocytes exposed to different ovarian stimulation protocols used in assisted reproductive technologies<sup>39</sup>.

Table 1

Biological process, functional enrichment, and cellular component of differentially expressed genes in superovulated null-NLRP2 oocyte versus superovulated wild-type using DAVID.

	Category ID	Term ID and Description	Count	%	P-Value
<b>Biological Process</b>	Neurogenesis (GO:0007399)		9	4.1	6.60E-03
	Differentiation (GO:0030154)	multicellular organism development (GO:0007275)	22	9.9	3.20E-03
		nervous system development (GO: 0007399)	12	5.4	3.60E-03
		Axon guidance (GO:0007411)	6	2.7	5.00E-02
<b>Molecular function</b>	Developmental protein (GO:0007275)	multicellular organism development (GO:0007275)	22	9.9	3.20E-03
		nervous system development (GO: 0007399)	12	5.4	3.60E-03
	Chaperone (KW-9992)	ATPase activity (GO:0016887)	9	4.1	6.70E-03
		Protein processing in endoplasmic reticulum (mmu04141)	7	3.2	1.20E-02
		positive regulation of telomerase activity (GO:0051973)	3	1.4	4.30E-02
		COP9 signalosome (GO:0008180)	3	1.4	4.30E-02
<b>Cellular Component</b>	Cytoplasm (KW-0963)	cytoplasm (KW-0963)	92	41.4	1.30E-03
		cytosol (GO:0005829)	57	25.7	3.40E-03
	Tight junction (KW-0796)	Cell adhesion molecules (mmu04514)	8	3.6	3.10E-03
		Tight junction (KW-0796)	7	3.2	1.00E-02
		bicellular tight junction (GO:0005923)	6	2.7	1.30E-02
		cell junction (GO:0030054)	16	7.2	3.50E-02
		cell-cell adhesion (GO:0098609)	6	2.7	4.50E-02
%: percentage of the identified DEGs out of the total genes in a pathway, FDR; false discovery rate					

Table 2

Differentially expressed genes involved in critical biological processes revealed by gene ontology enrichment analysis using WebGestalt.

Term ID	Term Description	Size	Expect	Enrichment Ratio	P-Value	FDR
R-MMU-392499	Metabolism of proteins	1619	16.1723865	2.287850342	1.65E-06	0.012488707
GO:0022612	gland morphogenesis	143	1.42844427	7.000623139	1.79E-06	0.012488707
R-MMU-597592	Post-translational protein modification	1321	13.1956285	2.425045533	2.80E-06	0.012970274
GO:0048667	cell morphogenesis involved in neuron differentiation	560	5.59390763	3.396552334	3.71E-06	0.012970274
GO:0007409	axonogenesis	418	4.17545248	3.831920034	5.00E-06	0.013338677
GO:0120036	plasma membrane bounded cell projection organization	1434	14.3243992	2.303761548	5.72E-06	0.013338677
GO:0034613	cellular protein localization	1587	15.8527346	2.207820971	7.27E-06	0.014521052
GO:0070727	cellular macromolecule localization	1597	15.9526259	2.193996169	8.33E-06	0.014562697
GO:0030030	cell projection organization	1473	14.7139749	2.242765824	1.00E-05	0.01556247
GO:0048812	neuron projection morphogenesis	610	6.09336366	3.118146405	1.25E-05	0.016021539
Size; total number of genes present in a pathway, Expect; Number of categories expected from set cover, Enrichment Ratio; number of observed divided by the number of expected genes from each GO category in the gene list, FDR; false discovery rate						

Table 3

Differentially expressed genes involved in critical biological processes revealed by gene ontology enrichment analysis using STRING.

Term ID	Term Description	Observed Gene Count	Background Gene Count	Strength	FDR
GO:0022612	Gland morphogenesis	11	123	0.94	0.0016
GO:0065007	Biological regulation	147	10591	0.13	0.0016
GO:0050794	Regulation of cellular process	135	9541	0.14	0.0023
GO:0007409	Axonogenesis	16	351	0.65	0.0024
GO:0048812	Neuron projection morphogenesis	19	479	0.59	0.0024
GO:0050789	Regulation of biological process	139	9973	0.13	0.0024
GO:0048667	Cell morphogenesis involved in neuron differentiation	17	440	0.58	0.0055
GO:0090287	Regulation of cellular response to growth factor stimulus	13	277	0.66	0.0097
GO:0007275	Multicellular organism development	79	4921	0.19	0.0112
GO:0030182	Neuron differentiation	27	1056	0.4	0.0136
Strength; probability of finding the linked proteins within the same KEGG pathway, FDR; false discovery rate					
<b>Supplementary Information</b>					

Both WebGestalt and STRING analysis revealed that gland morphogenesis had the highest enrichment ratio with a false discovery rate (FDR) of 0.01. Among the genes annotated to gland morphogenesis were *Notch2*, *Ctnnd1*, and *Tet2*, which have higher expression in *Nlrp2*-null oocyte pools. These genes are unique because of their known function and involvement in mouse oocyte growth and embryonic development<sup>40-46</sup>. qRT-PCR confirmed their upregulation on independently collected oocyte pools (Fig. 3a-c) (Primers are listed in Supplementary Table 2). TET2 is essential to survival during the early postnatal period<sup>47</sup>. *Tet2* deficiency decreases oocyte development and quality and accelerates age-associated infertility<sup>41</sup>. *Tet1-3* deficient embryos arrest at the two-cell stage; the most severe phenotype is linked to *Tet2*<sup>48</sup>. NOTCH2 regulates ovarian follicle formation and coordinates follicular growth<sup>48</sup>, and *Notch2* deficiency results in embryonic death by E11.5, which is related to placental defects<sup>42</sup>. CTNND1 plays a crucial role in the developing mouse brain such that its ablation results in aberrant embryonic morphology and in defective neurogenesis and neural tube formation in mid-gestation embryos<sup>43,49</sup>. While we do not yet know which precise mechanisms underlie the transcriptome changes in *Nlrp2*-null oocytes, these genes' overexpression may be compensatory responses to impaired oocyte and embryo development.

## Network analysis shows enrichment for proteins that contribute to post-translational methylation

We then used the STRING online database<sup>38</sup> to identify proteins that interact with or are functionally associated with proteins that upregulated DEGs encode. When we used the highest confidence setting in STRING, one "Annotated Keyword" from the UniProt database, methylation (KW-0488, gene count = 16, FDR = 0.026)—which is a subcategory of post-translational modification (PTM; KW-9991)—was enriched. We then used Cytoscape<sup>50</sup> to extract and visualize the gene network based on this STRING protein interaction enrichment (Fig. 4a). We further expanded this network to include adjacent genes, which yielded 75 upregulated genes (Fig. 4b). This expanded network also contains *Notch2*, *Ctnnd1*, and *Tet2*, enriched genes which we found annotated to the gland morphogenesis GO term. The expanded network also contains *Kdm1b*, which had higher expression in *Nlrp2*-null oocytes and was confirmed by qRT-PCR (Fig. 3d). *Kdm1b* is also the highest differentially expressed gene in the enriched "metabolism of proteins" pathway. This KDM1B enrichment is of interest because it is a H3K4 histone demethylase that

is required during oocyte development for the establishment of DNA methylation marks at CpG islands, including at imprinted genes<sup>51</sup>. Oocytes from *Kdm1b*-null females have increased H3K4 methylation and fail to set up proper DNA methylation marks at some imprinted genes. *Kdm1b*-null mice pregnancies show severe placental defects and embryos with myriad developmental abnormalities<sup>51</sup>.

## Data analysis according to oocyte reference annotation identified many new transcripts

We next aligned our sequence reads to a previously reported *de novo* assembled reference mouse oocyte-specific transcriptome. This mouse oocyte-specific transcriptome was obtained using strand-specific deep RNA-seq with *de novo* transcriptome assembly at different follicular growth stages. It contains 82,939 transcripts corresponding to 39,099 expressed genes, more than half of which were not known prior to that study<sup>29</sup>. We mapped the reads to the oocyte-specific transcriptome and, by including minimum average read count of 10 in our samples, identified and further studied 18,430 transcripts. PCA analysis using these transcripts revealed larger variations among samples and showed that one *Nlrp2*-null sample did not cluster with the other *Nlrp2*-null samples (Fig. 5a-b). We therefore removed this sample, which resulted in three WT and three *Nlrp2*-null samples available for differential expression analysis. There were 228 transcripts with differential expression at FDR < 0.05 between oocyte pools from WT and *Nlrp2*-null females (Supplementary Table 3). Of these, 90 had lower expression and 138 had higher expression in *Nlrp2*-null mice oocytes (Fig. 5c). Since only 47.7% of the oocyte transcriptome corresponded to reference annotation<sup>29</sup>, we did not expect all 228 differentially expressed transcripts to correspond to known genes in the reference genome. To further understand these transcripts' characteristics as to known canonical functions, then, we inspected 228 differentially expressed transcripts' genomic alignment for known reference genes that have a transcription start site (TSS) located within 10Kb of the aligned oocyte-specific transcripts. This identified 159 known reference genes (Supplementary Table 4). WebGestalt GO enrichment analysis of the 159 genes showed that most of them are involved in the TGF-beta signaling pathway and in negatively regulating the hydrogen peroxide metabolic process.

## DEGs overlap with hypermethylated and hypomethylated domains

The average oocyte methylation level is ~40% with a bimodal distribution of CpG methylation and hypermethylated CpGs primarily located within some genes' transcribed regions<sup>52,53</sup>. Veselovska and colleagues recently defined the mouse oocyte transcriptome and demonstrated that transcription drives DNA methylation establishment in female germ cells. They further discovered that methylated CpG are not randomly distributed in oocytes but instead tend to cluster together, and defined 21,044 hypermethylated domains (HyperDs) and 25,165 hypomethylated domains (HypoDs) within the oocyte DNA methylome<sup>29</sup>. A HyperD is a region that, due to active transcription, acquires methylation on the gene body, while a HypoD is depleted of methylation because it lacks transcription<sup>29</sup>.

We first examined the overlap between HyperDs and HypoDs of genes with altered expression from RNA-Seq data alignment to the reference mouse genome (Fig. 6a, Supplementary Table 5). Of the 231 DEGs, 156 (68%) overlapped with HyperDs or HypoDs. Given the known correlation between gene transcription and DNA methylation at HyperDs, we next examined the relationship between transcript levels in *Nlrp2*-null versus WT oocytes and mapping to HyperDs. We found that 83 of 108 (77%) underexpressed genes and 55 of 123 (45%) overexpressed genes in *Nlrp2*-null oocytes overlap with HyperDs. It is significantly more likely for underexpressed genes to overlap with HyperDs than for overexpressed genes ( $p = 0.0043$ , Fisher's Exact test). In contrast, only 4 of the 108 (4%) underexpressed genes and 14 of the 123 (11%) overexpressed genes overlap with HypoDs.

Next, we analyzed HyperDs and HypoD overlap with DEGs identified from alignment to the oocyte reference transcriptome. Of the 228 DEGs, 127 (56%) overlapped with either HyperDs (89 transcripts) or HypoDs (38 transcripts) (Fig. 6b, Supplementary Table 6). We found that 51 of 90 (57%) underexpressed genes mapped to HyperDs compared to only 38 of 138 (28%) overexpressed genes. Again, it is much more likely for underexpressed genes to overlap with HyperDs than overexpressed genes ( $p = 0.0018$ , Fisher's Exact test). When we examined overlap with HypoDs, we found that 10 of 90 (11%) underexpressed genes and 28 of 138 (20%) overexpressed genes in *Nlrp2*-null oocytes overlapped with HypoDs. We do not have genome-wide

methylation profiling data on these oocytes, but considering that transcription drives methylation in oocytes, it will be interesting to see if methylation levels at the HyperDs and HypoDs correlate with their overlapping transcripts' over- and underexpression. Confirming this could provide mechanistic insight into the consequences of maternal *Nlrp2* loss on oocytes and, consequently, offspring DNA methylation patterns at specific loci.

## Discussion

In this study, we found that maternal loss of *Nlrp2* function, a gene that encodes an oocyte SCMC protein, causes altered levels of hundreds of transcripts in superovulated MII-stage oocytes. Considering that the zygote and early preimplantation embryo depend upon stored transcript action and the proteins expressed during oocyte development (until the zygotic genome is activated) for all their functions<sup>54</sup>, these results could elucidate the mechanisms by which disrupting the SCMC (through loss of a component protein) can profoundly affect the earliest embryonic development stages. The SCMC is conserved among mammals and essential for mammalian preimplantation development. In addition to the aforementioned biological processes that occur during the transition from oocyte to embryo, the SCMC affects epigenetic reprogramming and regulation of mRNA<sup>15</sup>. Yet, despite extensive research about the SCMC's involvement in essential processes, its function remains incompletely understood.

Women who carry a mutation in one of several genes encoding SCMC proteins are healthy but have an increased risk of embryonic lethality and reproductive failure. This failure is often due to early developmental arrest<sup>55</sup>. In addition to causing female infertility, mutations in these genes can also cause imprinting disorders. Mutations in some genes that encode SCMC proteins have been associated with multi-locus imprinting disturbance (MLID) and biparental complete hydatidiform mole (BiCHM)<sup>19,20,24,28</sup>. This suggests that SCMC proteins play a role in establishing and possibly maintaining differential DNA methylation at maternally imprinted loci.

Performing maternal knockouts of different genes that encode SCMC proteins in mice most frequently yields early embryo arrest but not major alterations in oogenesis<sup>15</sup>. Female mice lacking *Nlrp2* are subfertile; they experience early embryonic loss and produce fewer offspring that have wide-ranging developmental phenotypes and abnormal DNA methylation at imprinted loci<sup>16</sup>. To our knowledge, no studies assessing oocyte methylation and transcription content in these mouse models exist. However, one study on oocytes from a human patient with loss of *KHDC3L*—a SCMC protein associated with hydatidiform moles and MLID—revealed a genome-wide DNA methylation deficit in the *KHDC3L*-deficient oocytes. This led the study's authors to conclude that *KHDC3L* is indispensable for establishing *de novo* DNA methylation in the growing human oocyte<sup>23</sup>.

We next performed functional analysis to gain deeper insight into the DEGs' biological functions and construct dysregulated transcript networks. Conducting functional annotation using DAVID analysis revealed that Neurogenesis (GO:0007399) and Differentiation (GO:0030154) are the two most enriched biological processes. NLRP2 is expressed in the central nervous system and its inactivation affects the transcription of genes implicated in nervous system development<sup>56</sup>.

Chaperone (KW-9992) is the most significantly enriched molecular function among DEGs. This function includes protein processing in the endoplasmic reticulum (mmu04141), a process that has been implicated in the oocyte-to-embryo transition upon the change of endoplasmic reticulum architecture<sup>57</sup>. The SCMC proteins NLRP5, OOEP, and PADI6 colocalize with oocyte cytoplasmic lattices (which regulate oocyte maturation) and microtubule dynamics and store maternal protein synthesis machinery components, including ribosomes, to contribute to the early embryo. CPL formation and organelle distribution within the oocyte, including the endoplasmic reticulum, also require these SCMC proteins<sup>4,12,14,58,59</sup>. Since NLRP2 is an SCMC protein that interacts with OOEP and NLRP5<sup>16</sup>, it is possible that it also directly interacts or physically associates with CPLs, and that the absence of these interactions in oocytes without NLRP2 disrupts the CPLs, but this requires further investigation.

In female germ cells, transcription drives most of the *de novo* DNA methylation establishment<sup>32,33,60</sup>. Therefore, any change in gene expression that occurs during oocyte maturation could alter the DNA methylation pattern. Another important event that occurs in a growing oocyte during *de novo* DNA methylation establishment is the exclusion of methylated H3K4. This histone mark must be removed in order to recruit DNA methyltransferases 3A/3L. KDM1B is the major factor that removes methylated

H3K4 in mouse oocytes and is essential to most imprinted genes and CpG islands (CGIs) that acquire methylation in oocytes<sup>61</sup>. The failure to set up DNA methylation marks at multiple maternally imprinted loci in KDM1B-deficient female oocytes confirms KDM1B's role in this process<sup>51</sup>.

Next, to better understand KDM1B upregulation's significance in *Nlrp2*-null cells and investigate its possible connection to altered DNA methylation, we examined the expression changes of genes that map to annotated oocyte HyperDs and HypoDs' genomic regions. Because active transcription drives DNA methylation in oocytes, we hypothesize that altered transcription of genes annotated to HyperDs and HypoDs can change those domains' methylation status and cause an altered HyperD and HypoD distribution in *Nlrp2*-null female oocytes (Fig. 6). Specifically, reduced transcription of genes that map to HyperDs could cause those HyperDs to acquire less or no methylation, turning them into HypoDs. Conversely, increased transcription of genes that map to HypoDs could cause those HypoDs to acquire more methylation, turning them into HyperDs. We observed that, among the four possible overlaps—(1) underexpressed DEGs with HyperDs, (2) overexpressed DEGs with HyperDs, (3) underexpressed DEGs with HypoDs, and (4) overexpressed DEGs with HypoDs—the most significant was underexpressed DEGs and HyperDs in both analyses (83 for the reference genome and 51 for the oocyte reference transcriptome). We therefore propose that less expression of transcripts that map to annotated HyperDs in *Nlrp2*-null oocytes could result losing methylation in those HyperDs. Although we do not have DNA methylation or histone profiling data for these oocytes, recent methylation profiling data from human oocytes deficient in KHDC3L revealed a genome-wide DNA methylation deficit<sup>23</sup>. It is therefore plausible that deleting NLRP2 and other SCMC members causes the same deficiency. We further speculate that KDM1B upregulation in *Nlrp2*-null oocytes might be a compensatory mechanism designed to balance methylation loss at these HyperDs. We will need to do more methylation and histone profiling to test these possibilities.

One of our study's limitations is that we generated our data from transcriptionally silent MII oocytes. In these cells, the gamete-specific DNA methylation patterns are already established and there is no active transcription. Moreover, we collected the oocytes for this study from superovulated mice and there is increasing evidence that superovulation alters DNA methylation and gene expression<sup>39,62</sup>. Ovarian stimulation also impairs oocyte/embryo quality, decreases the implantation rate, and increases embryo aneuploidy and fetal malformation rates<sup>63–65</sup>. Superovulated mouse oocytes are less able to perform endocytosis and fertilizing them produces blastocysts with fewer microvilli than their naturally fertilized counterparts<sup>66</sup>. It will therefore be important to perform similar studies on oocytes collected without prior superovulation and closer to the timing of methylation establishment.

In conclusion, this study shows that maternal NLRP2 loss has widespread consequences on mature oocyte transcriptomes and, therefore, reproductive outcomes and embryo development. It also illuminates possible underlying mechanisms that are worthy of further investigation. We are currently using new technology to perform small cell-number and single-cell combined RNA-sequencing and DNA methylation profiling in order to analyze transcriptome and methylome at early oocyte development stages and in cleavage-stage embryos produced from natural fertilization without superovulation.

## Materials And Methods

All experiments were approved by the Baylor College of Medicine (BCM) Institutional Animal Care and Use Committee (protocol AN-2035) All experiments were conducted according to institutional and governmental regulations concerning the ethical use of animals and American Veterinary Medical Association (AVMA) and ARRIVE Guidelines were followed. All animal facilities are approved by the Association for Assessment and Accreditation for Laboratory Animal Care International (AAALAC).

### 1. Animals, superovulation, and sample collection

Experiments were performed on the previously described *Nlrp2*-null (*Nlrp2<sup>tm1a/tm1a</sup>*) mouse model on a C57BL6/J background<sup>16</sup>. Superovulation was induced in four week old WT and *Nlrp2*-null mice by intraperitoneal injection of 5U of pregnant mare's serum gonadotropin (PMSG; Fisher Scientific, USA) followed by injection of 5U of human chorionic gonadotropin (hCG; EMD Millipore, USA) 48 h later. The following day at midday, COCs were collected from the ampulla of the oviduct. The same timing was observed for all animals. Denuded oocytes were prepared by treating COCs with 3 mg/ml hyaluronidase (Sigma-Aldrich, USA) for 2 minutes at room temperature. Oocytes from 3–4 mice of the same genotype were pooled to obtain pools of approximately 150

oocytes in each sequenced RNA sample. RNA was isolated from four *Nlrp2*-null and three WT oocyte pools using the Qiagen miRNeasy kit (QIAGEN, US) and used for the preparation of RNA-Seq libraries.

## 2. Library preparation and RNA sequencing

Library preparation and sequencing were done at the Genomic and RNA Profiling core at BCM. Libraries were prepared with the NuGEN RNA-Seq library preparation protocol. Briefly, purified double-stranded cDNA was generated from approximately 20 ng of total RNA and amplified using both oligo d(T) and random primers. Five hundred nanograms of each sample's ds-cDNA were sheared using the Covaris S2 focused-ultrasonicator (Covaris, USA) to a target size of 400 bp. A double-stranded DNA library was then generated from 1 µg of sheared, double-stranded cDNA, preparing the fragments for hybridization to the flowcell. Using the concentration from the ViiA7™ qPCR machine, 14 pM of the equimolarly pooled library is loaded onto an Illumina HiSeq 2500 sequencing instrument (Illumina, USA). PhiX Control v3 adapter-ligated library is spiked-in at 2% to ensure balanced diversity and to monitor clustering and sequencing performance. A paired-end 100 cycle run is used to sequence the flowcell on a HiSeq Sequencing System in Rapid Mode with v2 chemistry. Bcls (Illumina sequencer's base call files) were demultiplexed and FASTQs generated using Illumina BaseSpace. The average depth of sequencing per sample was 125 million read pairs.

## 3. RNA-Seq data analyses

For each sample, about 100 million pairs of 100-bp paired-end reads were generated. Following the standard approach, 10 bp were from the 5' end of the raw reads to remove biases on certain nucleotides resulting from poor priming during library preparation. For the first analysis strategy, which aimed to determine the abundance of transcripts expressed from annotated genes in the reference mouse genome, trimmed reads were aligned to the *Mus musculus* genome (GRcm38, p6.VM24) using TopHat v2.0.9<sup>67</sup> with default parameters. The average mappability for the seven samples was 71.16% (70.40% – 71.90%). HTSeq<sup>68,69</sup> was used to obtain read counts. Differential expression analysis between *Nlrp2*-null and WT superovulated oocytes was carried out based on the read counts using the DESeq package in the R environment<sup>69</sup>. The genes with adjusted p-value < 0.05 were considered differentially expressed genes (DEGs).

For the second analysis strategy, which aimed to determine transcript abundance compared to a recently published oocyte reference transcriptome, raw reads were mapped to the oocyte-specific transcriptome reported by Veselovska et al.<sup>29</sup> using STAR (version 2.5.0a) with default parameters<sup>70</sup>. The average mappability of this reference oocyte transcriptome for the seven samples was 79.48% (79.01% – 80.065). Next, featureCounts (version 1.5.0-p1)<sup>71</sup> was used to quantify the reads for oocyte-specific transcripts based on the annotation Gene Transfer Format (GTF) file provided by Veselovska et al – presented in Additional file 5 from that paper-<sup>29</sup>. Based on the read counts, differential transcript analysis between *Nlrp2*-null and WT superovulated oocytes was performed using DESeq2 (version 1.22.2) in R<sup>72</sup>. We annotated the transcripts to their closest genes using HOMER<sup>73</sup>, and a gene is considered for following analyses if the transcript is within 10 kb upstream of the gene's transcription start site. For both strategies, the Principal Component Analysis (PCA) was carried out using the normalized read counts on all the genes or all the transcripts in the R environment.

## 4. GO and pathway enrichment

Function and pathway enrichment analysis was performed using three online tools to analyze the biological process, cell component, and molecular function of the DEGs; Database for Annotation, Visualization and Integrated Discovery (DAVID) (<https://david.ncifcrf.gov/home.jsp>), and the WEB-based Gene SeT AnaLysis Toolkit (WebGestalt Toolkit) (<http://www.webgestalt.org/>)<sup>74,75</sup>. The STRING (<https://string-db.org/>) online database was applied to obtain a description of know protein-protein interaction (PPI). Cytoscape software platform (<https://cytoscape.org/>) was used to visualize the network.

## 5. Validations by RT-qPCR

RNA samples used for validation were isolated from independent pools of superovulated oocytes and 500 ng of RNA was reverse transcribed into cDNA using the qScript cDNA SuperMix (Quanta Biosciences #95048). Quantitative RT-PCR of reverse-transcribed cDNAs was done with PerfeCTa® SYBR® Green FastMix ROX (Quanta Biosciences #95073) using the primers listed in Supplementary Table 2. Gene expression analysis was performed using the  $\Delta\Delta$ Ct method and normalized to the expression of *Rp19* mRNA.

## 6. Overlap of identified transcripts with oocyte hyper- and hypomethylated domains

Hypermethylated domains (HyperDs) and hypomethylated domains (HypoDs) identified in Veselovska et. al's study<sup>29</sup> were used as references. A gene is considered to fall into HyperDs/HypoDs domain if at least 50% of the gene body (from transcription start to transcription end) overlaps with the region. Similarly, a transcript is considered to be falling into the domain if a least 50% of the transcript overlaps with the region. Intersect function from bedtools (v2.25.0) was used to identify the overlaps.

### Declarations

**Acknowledgements:** This work was supported by grants R01HD092746 and P50HD103555 (for use of the administrative core), from the *Eunice Kennedy Shriver* National Institute of Child Health & Human Development of the National Institutes of Health. M.S. is supported by postdoctoral fellowship award from The Lalor Foundation, INC and by T32HD098068. This project was supported in part by the Genomic and RNA Profiling Core at Baylor College of Medicine with funding from the NIH NCI (P30CA125123) and CPRIT (RP200504) grants. The content is solely the responsibility of the authors and does not necessarily represent the official views of the National Institutes of Health.

**Author contributions statement:** SM, YWW and IV conceived the experiments; ZA, SM, IC, ETN performed experiments; YWW, ZL, IC, LS, MS analyzed data. ZA and IV wrote the manuscript. All authors contributed to manuscript editing. IV acquired funding and was responsible for overall oversight and final editing.

**Data availability statement:** Data is privately available as of (09/13) and will be updated to publicly available from the Gene Expression Omnibus (GEO) accession number: GSE213059; [https://urldefense.proofpoint.com/v2/url?u=https-3A\\_\\_www.ncbi.nlm.nih.gov\\_geo\\_query\\_acc.cgi-3Facc-3DGSE213059&d=DwIBAg&c=ZQs-KZ8oxEwOp81sqgiaRA&r=FSQHUjzldjQD5veAVXWk3-3CV1YgXGFN2iF4l8qSFWg&m=lcKKQtR18jOGKPA\\_9IngCgjYQLEl bubjW5VLxvAF89N9LOL8I5WJWFpUaWmiE9XM&s=eD0oXizM-E1qw6HbZZMEBBbei0z0clIGmyHexHq0Tag&e=](https://urldefense.proofpoint.com/v2/url?u=https-3A__www.ncbi.nlm.nih.gov_geo_query_acc.cgi-3Facc-3DGSE213059&d=DwIBAg&c=ZQs-KZ8oxEwOp81sqgiaRA&r=FSQHUjzldjQD5veAVXWk3-3CV1YgXGFN2iF4l8qSFWg&m=lcKKQtR18jOGKPA_9IngCgjYQLEl bubjW5VLxvAF89N9LOL8I5WJWFpUaWmiE9XM&s=eD0oXizM-E1qw6HbZZMEBBbei0z0clIGmyHexHq0Tag&e=); Enter token: utoxqqydtkdlyz into the box

**Competing Interests Statement:** The authors declare no competing financial interests.

### References

1. Wolf, J. B. & Wade, M. J. What are maternal effects (and what are they not)? *Philos Trans R Soc Lond B Biol Sci* **364**, 1107-1115, doi:10.1098/rstb.2008.0238 (2009).
2. Li, L., Baibakov, B. & Dean, J. A subcortical maternal complex essential for preimplantation mouse embryogenesis. *Dev Cell* **15**, 416-425, doi:10.1016/j.devcel.2008.07.010 (2008).
3. Lu, X., Gao, Z., Qin, D. & Li, L. A Maternal Functional Module in the Mammalian Oocyte-To-Embryo Transition. *Trends in molecular medicine* **23**, 1014-1023, doi:10.1016/j.molmed.2017.09.004 (2017).
4. Qin, D. *et al.* The subcortical maternal complex protein Nlrp4f is involved in cytoplasmic lattice formation and organelle distribution. *Development* **146**, doi:10.1242/dev.183616 (2019).
5. Peng, H. *et al.* Nlrp2, a maternal effect gene required for early embryonic development in the mouse. *PLoS One* **7**, e30344, doi:10.1371/journal.pone.0030344 (2012).
6. Gao, Z. *et al.* Zbed3 participates in the subcortical maternal complex and regulates the distribution of organelles. *J Mol Cell Biol* **10**, 74-88, doi:10.1093/jmcb/mjx035 (2018).
7. Tong, Z. B. *et al.* Mater, a maternal effect gene required for early embryonic development in mice. *Nat Genet* **26**, 267-268, doi:10.1038/81547 (2000).
8. Ohsugi, M., Zheng, P., Baibakov, B., Li, L. & Dean, J. Maternally derived FILIA-MATER complex localizes asymmetrically in cleavage-stage mouse embryos. *Development* **135**, 259-269, doi:10.1242/dev.011445 (2008).

9. Esposito, G. *et al.* Peptidylarginine deiminase (PAD) 6 is essential for oocyte cytoskeletal sheet formation and female fertility. *Mol Cell Endocrinol* **273**, 25-31, doi:10.1016/j.mce.2007.05.005 (2007).
10. Yu, X. J. *et al.* The subcortical maternal complex controls symmetric division of mouse zygotes by regulating F-actin dynamics. *Nat Commun* **5**, 4887, doi:10.1038/ncomms5887 (2014).
11. Zheng, P., Baibakov, B., Wang, X. H. & Dean, J. PtdIns(3,4,5)P3 is constitutively synthesized and required for spindle translocation during meiosis in mouse oocytes. *J Cell Sci* **126**, 715-721, doi:10.1242/jcs.118042 (2013).
12. Kim, B. *et al.* The role of MATER in endoplasmic reticulum distribution and calcium homeostasis in mouse oocytes. *Dev Biol* **386**, 331-339, doi:10.1016/j.ydbio.2013.12.025 (2014).
13. Fernandes, R. *et al.* NLRP5 mediates mitochondrial function in mouse oocytes and embryos. *Biol Reprod* **86**, 138, 131-110, doi:10.1095/biolreprod.111.093583 (2012).
14. Tashiro, F. *et al.* Maternal-effect gene *Ces5/Ooep/Moep19/Floped* is essential for oocyte cytoplasmic lattice formation and embryonic development at the maternal-zygotic stage transition. *Genes Cells* **15**, 813-828, doi:10.1111/j.1365-2443.2010.01420.x (2010).
15. Bebbere, D., Albertini, D. F., Coticchio, G., Borini, A. & Ledda, S. The subcortical maternal complex: emerging roles and novel perspectives. *Mol Hum Reprod* **27**, doi:10.1093/molehr/gaab043 (2021).
16. Mahadevan, S. *et al.* Maternally expressed NLRP2 links the subcortical maternal complex (SCMC) to fertility, embryogenesis and epigenetic reprogramming. *Sci Rep* **7**, 44667, doi:10.1038/srep44667 (2017).
17. Zheng, P. & Dean, J. Role of *Filia*, a maternal effect gene, in maintaining euploidy during cleavage-stage mouse embryogenesis. *Proc Natl Acad Sci U S A* **106**, 7473-7478, doi:10.1073/pnas.0900519106 (2009).
18. Andreasen, L., Christiansen, O. B., Niemann, I., Bolund, L. & Sunde, L. NLRP7 or KHDC3L genes and the etiology of molar pregnancies and recurrent miscarriage. *Mol Hum Reprod* **19**, 773-781, doi:10.1093/molehr/gat056 (2013).
19. Parry, D. A. *et al.* Mutations causing familial biparental hydatidiform mole implicate *c6orf221* as a possible regulator of genomic imprinting in the human oocyte. *Am J Hum Genet* **89**, 451-458, doi:10.1016/j.ajhg.2011.08.002 (2011).
20. Murdoch, S. *et al.* Mutations in *NALP7* cause recurrent hydatidiform moles and reproductive wastage in humans. *Nat Genet* **38**, 300-302 (2006).
21. Qian, J. *et al.* Biallelic *PADI6* variants linking infertility, miscarriages, and hydatidiform moles. *Eur J Hum Genet* **26**, 1007-1013, doi:10.1038/s41431-018-0141-3 (2018).
22. Sanchez-Delgado, M. *et al.* Absence of Maternal Methylation in Biparental Hydatidiform Moles from Women with NLRP7 Maternal-Effect Mutations Reveals Widespread Placenta-Specific Imprinting. *PLoS Genet* **11**, e1005644, doi:10.1371/journal.pgen.1005644 (2015).
23. Demond, H. *et al.* A KHDC3L mutation resulting in recurrent hydatidiform mole causes genome-wide DNA methylation loss in oocytes and persistent imprinting defects post-fertilisation. *Genome medicine* **11**, 84, doi:10.1186/s13073-019-0694-y (2019).
24. Docherty, L. E. *et al.* Mutations in NLRP5 are associated with reproductive wastage and multilocus imprinting disorders in humans. *Nat Commun* **6**, 8086, doi:10.1038/ncomms9086 (2015).
25. Meyer, E. *et al.* Germline mutation in NLRP2 (*NALP2*) in a familial imprinting disorder (Beckwith-Wiedemann Syndrome). *PLoS Genet* **5**, e1000423, doi:10.1371/journal.pgen.1000423 (2009).
26. Eggermann, T., Kadgien, G., Begemann, M. & Elbracht, M. Biallelic *PADI6* variants cause multilocus imprinting disturbances and miscarriages in the same family. *Eur J Hum Genet* **29**, 575-580, doi:10.1038/s41431-020-00762-0 (2021).
27. Eggermann, T. Maternal Effect Mutations: A Novel Cause for Human Reproductive Failure. *Geburtshilfe Frauenheilkd* **81**, 780-788, doi:10.1055/a-1396-4390 (2021).
28. Begemann, M. *et al.* Maternal variants in NLRP and other maternal effect proteins are associated with multilocus imprinting disturbance in offspring. *J Med Genet* **55**, 497-504, doi:10.1136/jmedgenet-2017-105190 (2018).
29. Veselovska, L. *et al.* Deep sequencing and de novo assembly of the mouse oocyte transcriptome define the contribution of transcription to the DNA methylation landscape. *Genome Biol* **16**, 209, doi:10.1186/s13059-015-0769-z (2015).

30. Okae, H. *et al.* Genome-wide analysis of DNA methylation dynamics during early human development. *PLoS Genet* **10**, e1004868, doi:10.1371/journal.pgen.1004868 (2014).
31. Gahurova, L. *et al.* Transcription and chromatin determinants of de novo DNA methylation timing in oocytes. *Epigenetics Chromatin* **10**, 25, doi:10.1186/s13072-017-0133-5 (2017).
32. Yan, R. *et al.* Decoding dynamic epigenetic landscapes in human oocytes using single-cell multi-omics sequencing. *Cell Stem Cell* **28**, 1641-1656 e1647, doi:10.1016/j.stem.2021.04.012 (2021).
33. Chotalia, M. *et al.* Transcription is required for establishment of germline methylation marks at imprinted genes. *Genes Dev* **23**, 105-117, doi:10.1101/gad.495809 (2009).
34. Huang da, W., Sherman, B. T. & Lempicki, R. A. Systematic and integrative analysis of large gene lists using DAVID bioinformatics resources. *Nature protocols* **4**, 44-57, doi:10.1038/nprot.2008.211 (2009).
35. Huang da, W., Sherman, B. T. & Lempicki, R. A. Bioinformatics enrichment tools: paths toward the comprehensive functional analysis of large gene lists. *Nucleic Acids Res* **37**, 1-13, doi:10.1093/nar/gkn923 (2009).
36. Sherman, B. T. *et al.* DAVID: a web server for functional enrichment analysis and functional annotation of gene lists (2021 update). *Nucleic Acids Res* **50**, doi:10.1093/nar/gkac194 (2022).
37. Liao, Y., Wang, J., Jaehnig, E. J., Shi, Z. & Zhang, B. WebGestalt 2019: gene set analysis toolkit with revamped UIs and APIs. *Nucleic Acids Res* **47**, W199-W205, doi:10.1093/nar/gkz401 (2019).
38. Szklarczyk, D. *et al.* The STRING database in 2021: customizable protein-protein networks, and functional characterization of user-uploaded gene/measurement sets. *Nucleic Acids Res* **49**, D605-D612, doi:10.1093/nar/gkaa1074 (2021).
39. Saenz-de-Juano, M. D. *et al.* Genome-wide assessment of DNA methylation in mouse oocytes reveals effects associated with in vitro growth, superovulation, and sexual maturity. *Clin Epigenetics* **11**, 197, doi:10.1186/s13148-019-0794-y (2019).
40. Vanorny, D. A., Prasasya, R. D., Chalpe, A. J., Kilen, S. M. & Mayo, K. E. Notch signaling regulates ovarian follicle formation and coordinates follicular growth. *Mol Endocrinol* **28**, 499-511, doi:10.1210/me.2013-1288 (2014).
41. Wang, X. *et al.* PROSER1 mediates TET2 O-GlcNAcylation to regulate DNA demethylation on UTX-dependent enhancers and CpG islands. *Life Sci Alliance* **5**, doi:10.26508/lsa.202101228 (2022).
42. Hamada, Y. *et al.* Notch2 is required for formation of the placental circulatory system, but not for cell-type specification in the developing mouse placenta. *Differentiation* **75**, 268-278, doi:10.1111/j.1432-0436.2006.00137.x (2007).
43. Pieters, T., Sanders, E., Tian, H., van Hengel, J. & van Roy, F. Neural defects caused by total and Wnt1-Cre mediated ablation of p120ctn in mice. *BMC Dev Biol* **20**, 17, doi:10.1186/s12861-020-00222-4 (2020).
44. Johnson, J., Espinoza, T., McGaughey, R. W., Rawls, A. & Wilson-Rawls, J. Notch pathway genes are expressed in mammalian ovarian follicles. *Mech Dev* **109**, 355-361, doi:10.1016/s0925-4773(01)00523-8 (2001).
45. Hernandez-Martinez, R., Ramkumar, N. & Anderson, K. V. p120-catenin regulates WNT signaling and EMT in the mouse embryo. *Proc Natl Acad Sci U S A* **116**, 16872-16881, doi:10.1073/pnas.1902843116 (2019).
46. Dawlaty, M. M. *et al.* Combined deficiency of Tet1 and Tet2 causes epigenetic abnormalities but is compatible with postnatal development. *Dev Cell* **24**, 310-323, doi:10.1016/j.devcel.2012.12.015 (2013).
47. Shide, K. *et al.* TET2 is essential for survival and hematopoietic stem cell homeostasis. *Leukemia* **26**, 2216-2223, doi:10.1038/leu.2012.94 (2012).
48. Arand, J. *et al.* Tet enzymes are essential for early embryogenesis and completion of embryonic genome activation. *EMBO Rep* **23**, e53968, doi:10.15252/embr.202153968 (2022).
49. Elia, L. P., Yamamoto, M., Zang, K. & Reichardt, L. F. p120 catenin regulates dendritic spine and synapse development through Rho-family GTPases and cadherins. *Neuron* **51**, 43-56, doi:10.1016/j.neuron.2006.05.018 (2006).
50. Shannon, P. *et al.* Cytoscape: a software environment for integrated models of biomolecular interaction networks. *Genome Res* **13**, 2498-2504, doi:10.1101/gr.1239303 (2003).
51. Ciccone, D. N. *et al.* KDM1B is a histone H3K4 demethylase required to establish maternal genomic imprints. *Nature* **461**, 415-418, doi:10.1038/nature08315 (2009).

52. Kobayashi, H. *et al.* Contribution of intragenic DNA methylation in mouse gametic DNA methylomes to establish oocyte-specific heritable marks. *PLoS Genet* **8**, e1002440, doi:10.1371/journal.pgen.1002440 (2012).
53. Shirane, K. *et al.* Mouse oocyte methylomes at base resolution reveal genome-wide accumulation of non-CpG methylation and role of DNA methyltransferases. *PLoS Genet* **9**, e1003439, doi:10.1371/journal.pgen.1003439 (2013).
54. Kobayashi, H., Nagao, K. & Nakajima, K. (2012).
55. Alazami, A. M. *et al.* TLE6 mutation causes the earliest known human embryonic lethality. *Genome Biol* **16**, 240, doi:10.1186/s13059-015-0792-0 (2015).
56. Sun, X. *et al.* NLRP2 is highly expressed in a mouse model of ischemic stroke. *Biochemical and biophysical research communications* **479**, 656-662, doi:10.1016/j.bbrc.2016.09.157 (2016).
57. Israel, S. *et al.* An integrated genome-wide multi-omics analysis of gene expression dynamics in the preimplantation mouse embryo. *Sci Rep* **9**, 13356, doi:10.1038/s41598-019-49817-3 (2019).
58. Kan, R. *et al.* Regulation of mouse oocyte microtubule and organelle dynamics by PADI6 and the cytoplasmic lattices. *Dev Biol* **350**, 311-322, doi:10.1016/j.ydbio.2010.11.033 (2011).
59. Longo, M., Boiani, M., Redi, C. & Monti, M. Cytoplasmic lattices are not linked to mouse 2-cell embryos developmental arrest. *Eur J Histochem* **62**, doi:10.4081/ejh.2018.2972 (2018).
60. Gu, C., Liu, S., Wu, Q., Zhang, L. & Guo, F. Integrative single-cell analysis of transcriptome, DNA methylome and chromatin accessibility in mouse oocytes. *Cell Res* **29**, 110-123, doi:10.1038/s41422-018-0125-4 (2019).
61. Stewart, K. R. *et al.* Dynamic changes in histone modifications precede de novo DNA methylation in oocytes. *Genes Dev* **29**, 2449-2462, doi:10.1101/gad.271353.115 (2015).
62. Uysal, F., Ozturk, S. & Akkoyunlu, G. Superovulation alters DNA methyltransferase protein expression in mouse oocytes and early embryos. *J Assist Reprod Genet* **35**, 503-513, doi:10.1007/s10815-017-1087-z (2018).
63. Huo, Y. *et al.* Single-cell DNA methylation sequencing reveals epigenetic alterations in mouse oocytes superovulated with different dosages of gonadotropins. *Clin Epigenetics* **12**, 75, doi:10.1186/s13148-020-00866-w (2020).
64. Lin, J. *et al.* Expanding the genetic and phenotypic spectrum of female infertility caused by TLE6 mutations. *J Assist Reprod Genet* **37**, 437-442, doi:10.1007/s10815-019-01653-0 (2020).
65. Ertzeid, G. & Storeng, R. The impact of ovarian stimulation on implantation and fetal development in mice. *Hum Reprod* **16**, 221-225, doi:10.1093/humrep/16.2.221 (2001).
66. Lee, M. *et al.* Adverse Effect of Superovulation Treatment on Maturation, Function and Ultrastructural Integrity of Murine Oocytes. *Mol Cells* **40**, 558-566, doi:10.14348/molcells.2017.0058 (2017).
67. Kim, D. *et al.* TopHat2: accurate alignment of transcriptomes in the presence of insertions, deletions and gene fusions. *Genome Biol* **14**, R36, doi:10.1186/gb-2013-14-4-r36 (2013).
68. Anders, S., Pyl, P. T. & Huber, W. HTSeq—a Python framework to work with high-throughput sequencing data. *Bioinformatics* **31**, 166-169, doi:10.1093/bioinformatics/btu638 (2015).
69. Anders, S. & Huber, W. Differential expression analysis for sequence count data. *Genome Biol* **11**, R106, doi:10.1186/gb-2010-11-10-r106 (2010).
70. Dobin, A. *et al.* STAR: ultrafast universal RNA-seq aligner. *Bioinformatics* **29**, 15-21, doi:10.1093/bioinformatics/bts635 (2013).
71. Liao, Y., Smyth, G. K. & Shi, W. featureCounts: an efficient general purpose program for assigning sequence reads to genomic features. *Bioinformatics* **30**, 923-930, doi:10.1093/bioinformatics/btt656 (2014).
72. Love, M. I., Huber, W. & Anders, S. Moderated estimation of fold change and dispersion for RNA-seq data with DESeq2. *Genome Biol* **15**, 550, doi:10.1186/s13059-014-0550-8 (2014).
73. Heinz, S. *et al.* Simple combinations of lineage-determining transcription factors prime cis-regulatory elements required for macrophage and B cell identities. *Mol Cell* **38**, 576-589, doi:10.1016/j.molcel.2010.05.004 (2010).
74. Wang, J., Duncan, D., Shi, Z. & Zhang, B. WEB-based GEne SeT Analysis Toolkit (WebGestalt): update 2013. *Nucleic Acids Res* **41**, W77-83, doi:10.1093/nar/gkt439 (2013).

## Figures

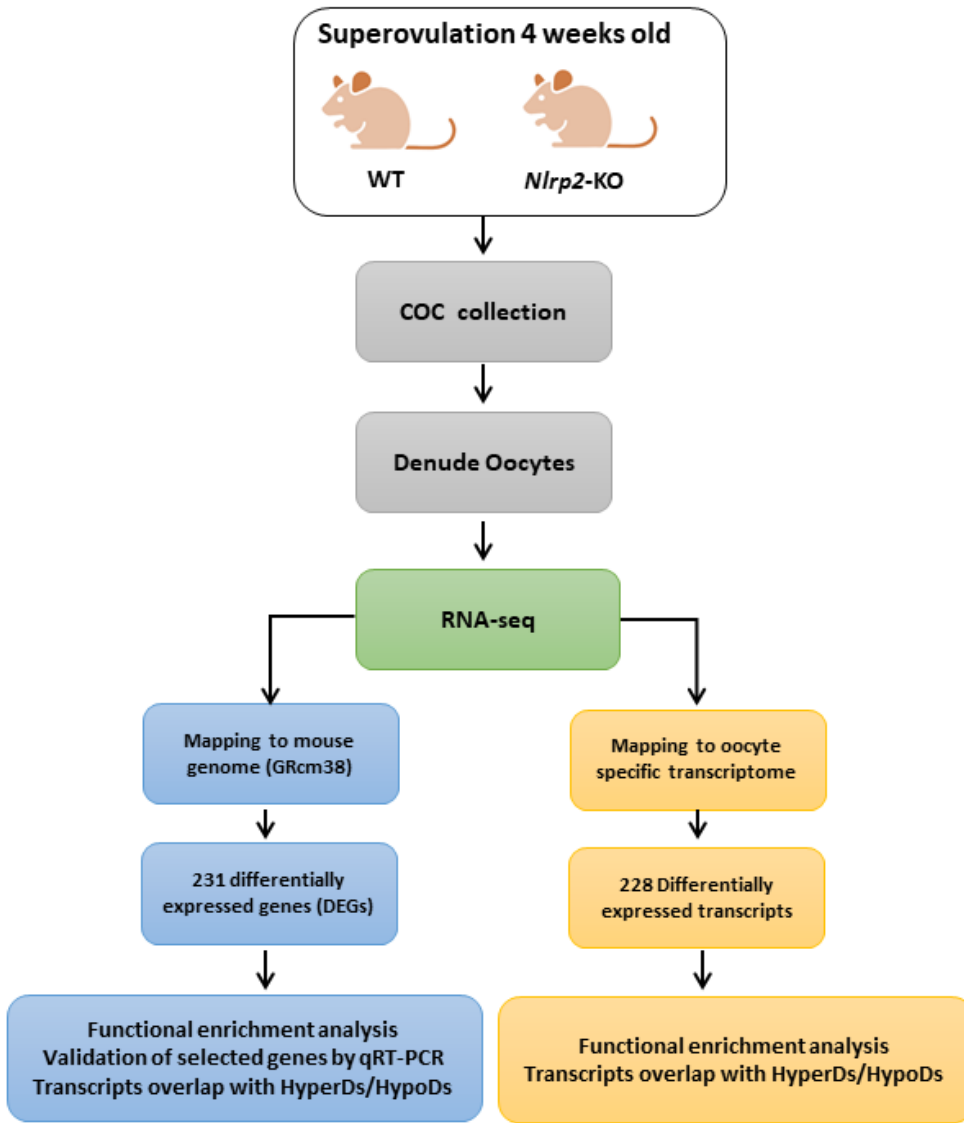


**Figure 1**

**Experimental design:** Four week old WT and *Nlrp2*-KO females were superovulated. The following day Cumulus oocyte complexes (COCs) were collected from the ampulla of the oviduct. Total RNA sequencing was performed on denuded oocytes. **Left**, route represents the first strategy, in which reads are mapped to the mouse reference genome and **right**, route represents the second strategy, in which reads are mapped to the mouse oocyte specific transcriptome.

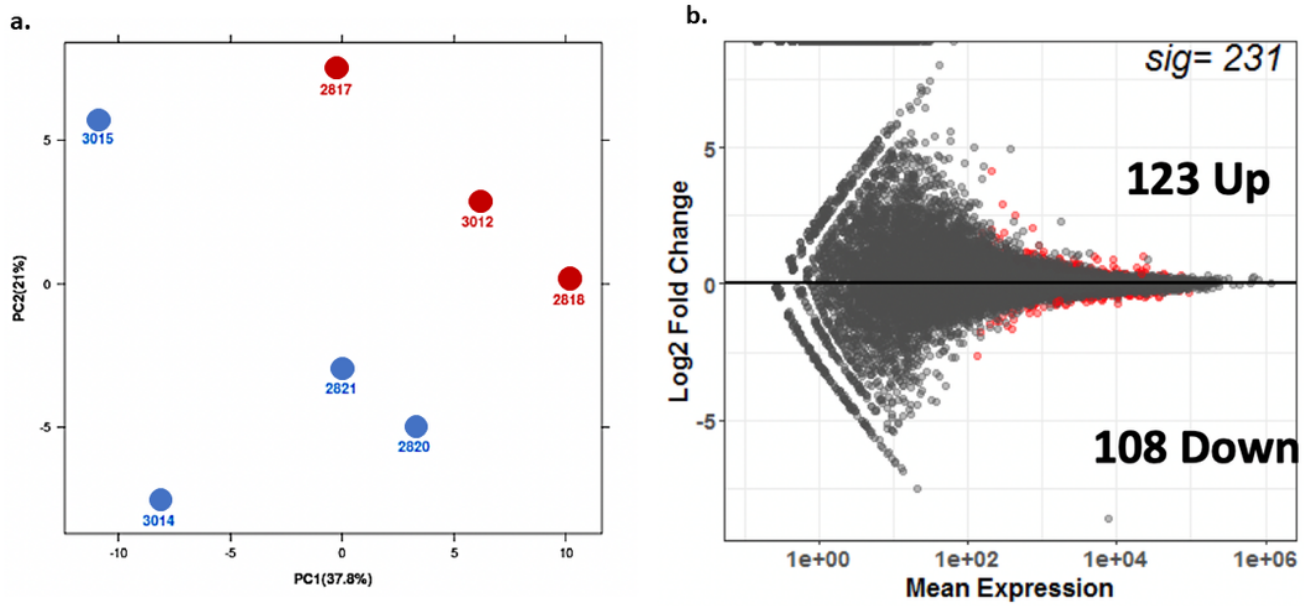


**Figure 2**

**a. Principal component analysis:** Normalized transcript counts from wild-type oocyte pools (WT; red) and *Nlrp2*-null oocyte pools (NULL; blue) cluster separately. **b. MA plot:** representing the Log<sub>2</sub> Fold Change (Y-axis) versus normalized mean expression (X-axis) between WT and *Nlrp2*-null samples. Unchanged genes (Grey), Differentially expressed genes (DEGs) (Red), adjusted p-value < 0.05.

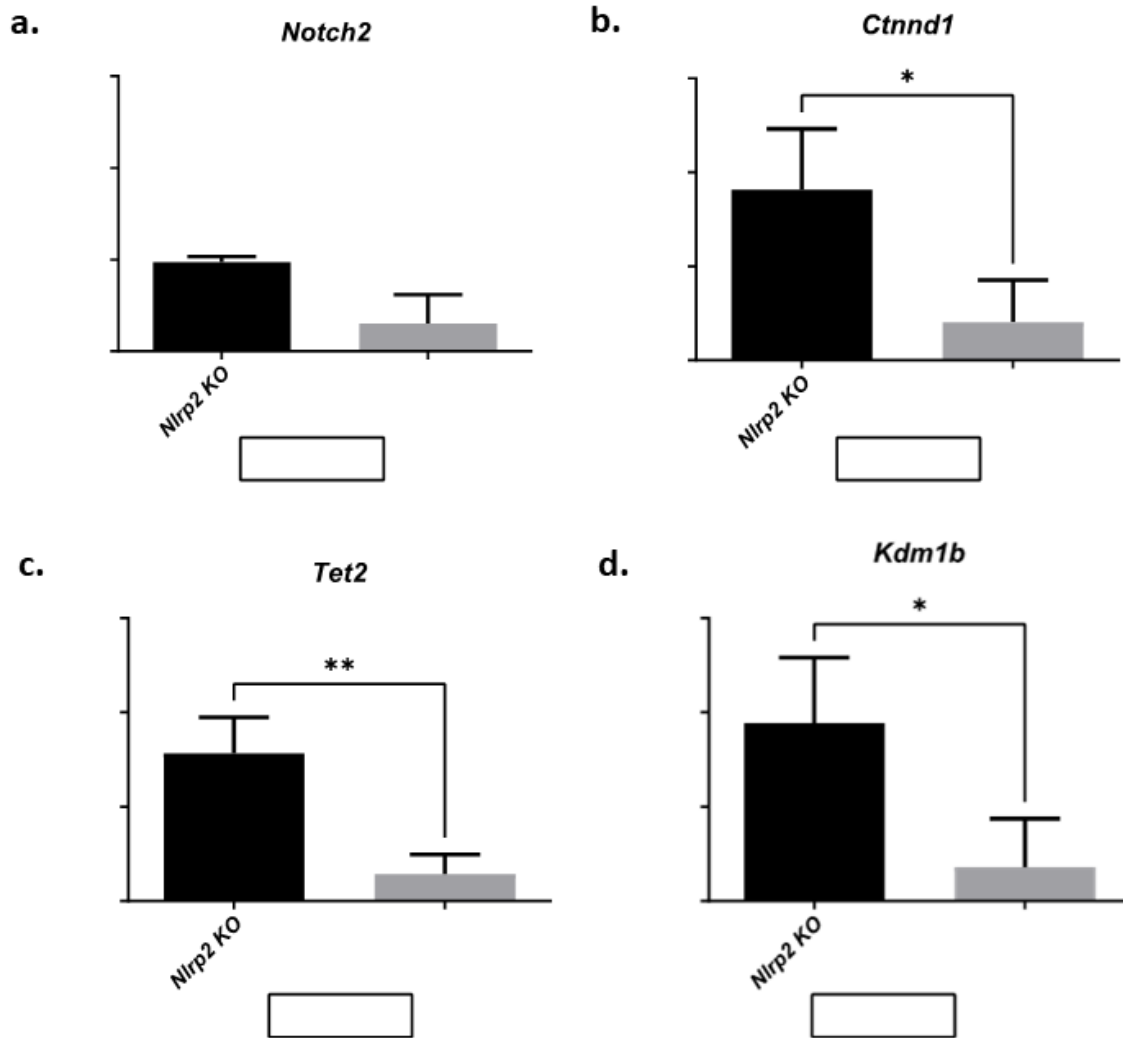


**Figure 3**

qRT-PCR confirmation of selected upregulated genes: a. *Notch2*; b. *Ctnnd1*; c. *Tet2*; d. *Kdm1b*. Gene expression was normalized to oocyte housekeeping gene *Rpl19*;

\*:  $p < 0.05$ ; \*\*:  $p < 0.01$ .

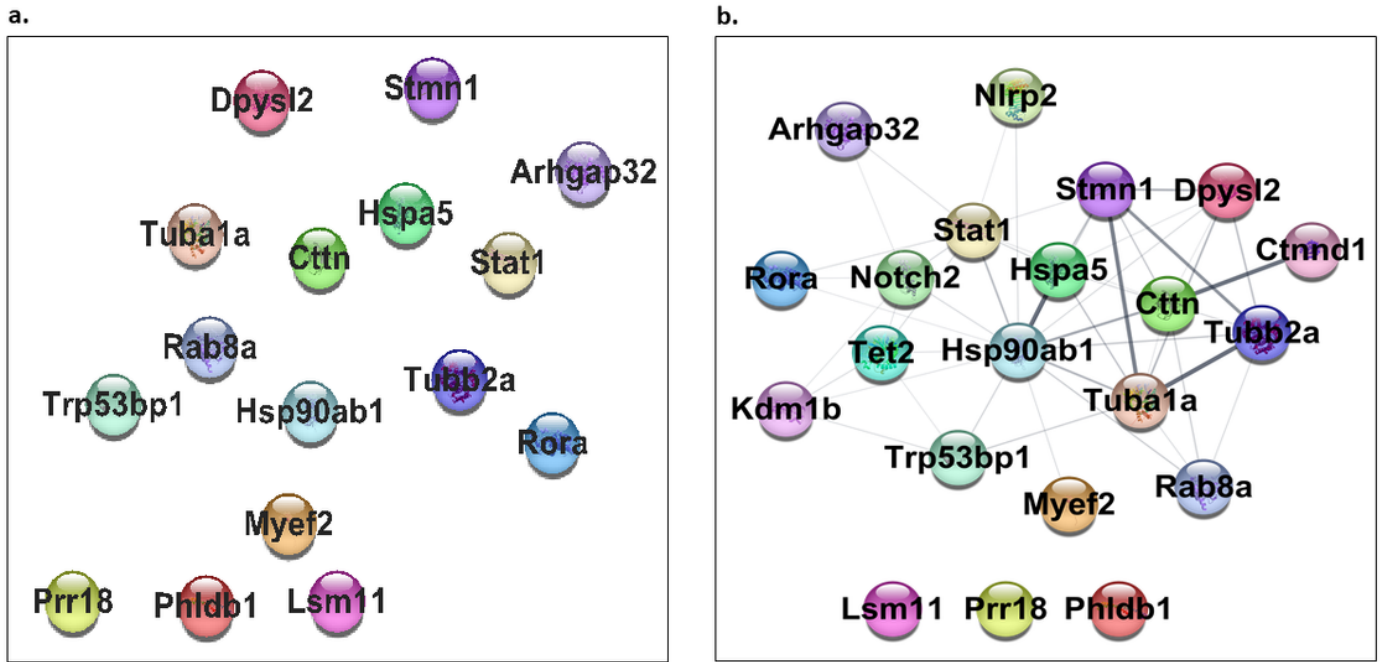


Figure 4

**Gene Network analysis:** **a.** Gene network based on STRING enrichment for methylation of the upregulated DEGs. **b.** Genes network based on STRING enrichment for methylation of the upregulated DEGs and the selected genes for qRT-PCR.

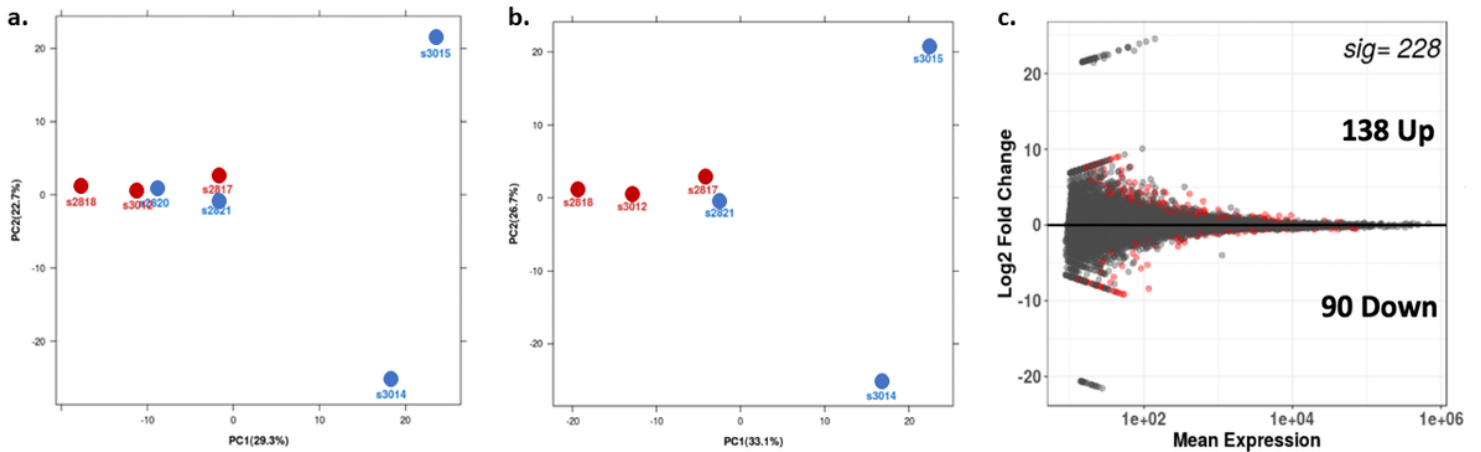


Figure 5

**Principal component analysis:** **a.** Normalized transcript counts from wild-type oocyte pools (WT; Red) and *Nlrp2*-null oocyte pools (NULL; Blue). **b.** PCA after removal of sample s2820. **c.** **MA plot** representing the Log<sub>2</sub> Fold Change (Y-axis) versus normalized mean expression (X-axis) between WT and *Nlrp2*-null samples compared to reference oocyte transcriptome<sup>29</sup>. Unchanged genes (Grey), Differentially expressed genes (DEGs) (Red), adjusted p-value < 0.05.

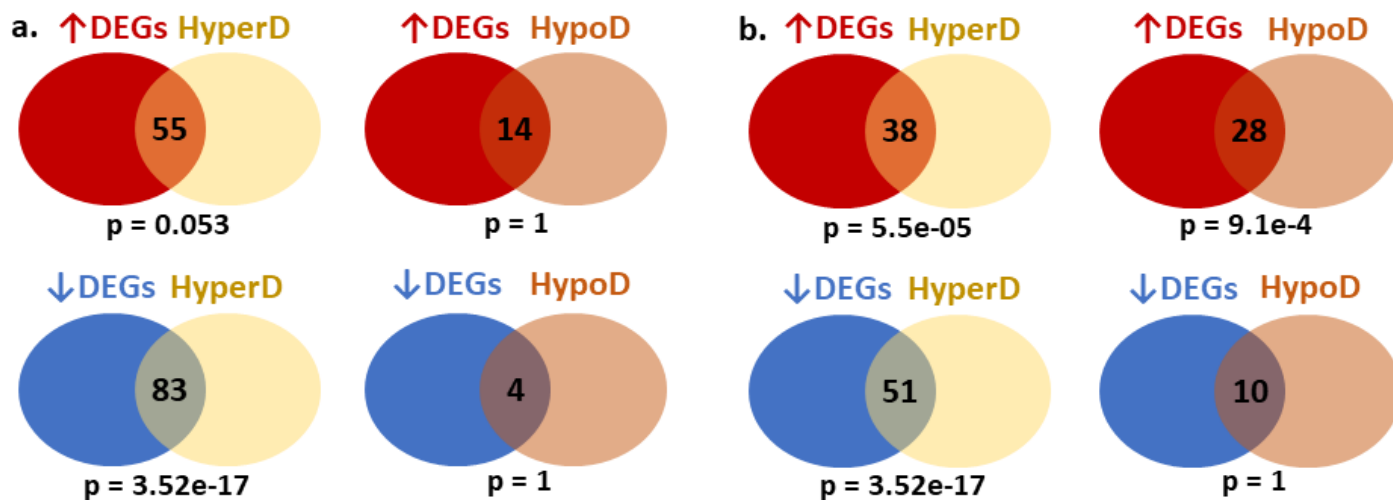


Figure 6

**Overlap of differentially expressed genes (DEGs) with hyper- and hypomethylated oocyte domains.** **a.** Overlap of DEGs found when RNA-Seq data were aligned to the reference genome. **b.** Overlap of DEGs found when RNA-Seq data were aligned to the reference oocyte transcriptome. Top venn-diagrams for each panel represent overlap of overexpressed DEGs with hypermethylated domains (HyperD) and Hypomethylated domains (HypoD) and bottom panel represent overlap of underexpressed DEGs with hypermethylated domains (HyperD) and Hypomethylated domains (HypoD), hypergeometric test;  $p < 0.05$ .

## Supplementary Files

This is a list of supplementary files associated with this preprint. Click to download.

- [S.Table1.xlsx](#)
- [S.Table2.xlsx](#)
- [S.Table3.xlsx](#)
- [S.Table4.xlsx](#)
- [S.Table5.xlsx](#)
- [S.Table6.xlsx](#)